

Radiative corrections in nucleon time-like form factors measurements

Jacques Van de Wiele¹ and Saro Ong^{1,2}

¹ Institut de Physique Nucléaire, IN2P3-CNRS, Université de Paris-Sud, 91406 Orsay Cedex, France.

² Université de Picardie Jules Verne, F-80000 Amiens, France

Received: date / Revised version: date

Abstract. The completely general radiative corrections to lowest order, including the final and initial state radiations, are studied in proton-antiproton annihilation into an electron-positron pair. Numerical estimates have been made in a realistic configuration of the PANDA detector at FAIR for the proton time-like form factors measurements.

PACS. 13.75.Cs Nucleon-nucleon interactions – 13.40.Gp Electromagnetic form factors

1 Introduction.

Precise polarization measurements of the proton electromagnetic form factor [1] confirm the Q^2 dependence up to $Q^2 = 8.5 \text{ GeV}^2$, of the ratio $R = \mu G_E / G_M$ (where μ is the proton's magnetic moment and G_E and G_M are the electric and magnetic proton form factors) showing an approximately linear decrease of R with Q^2 . This fact is in disagreement with results obtained from a new Rosenbluth cross section measurement [2] and suggests that the source of the discrepancy is not simply experimental. Recently, there has been a revival of interest in this subject [3]. Some theoretical works [4-6] have investigated the two-photon exchange corrections to the lowest order QED. This effect has been shown to resolve partially the discrepancy [3,7]. It is well established that the Rosenbluth method is much more sensitive to radiative corrections than the polarization method. Until now, intense theoretical activities to evaluate the radiative corrections to elastic electron-proton scattering, which include higher order radiative corrections [8,9] or model-dependent box diagram calculation [10], incorporating the nucleon's substructure, are not able to draw a definitive conclusion on this discrepancy. We should note that two-photon exchange corrections are small in general and at a 1% level for a large class of experiments [3]. With this renewal of interest, the importance of theoretical descriptions of nucleon form

factors in the space-like and also in the time-like region is emphasized.

In principle, time-like form factors can be evaluated from the space-like equivalents by means of dispersion relations. The ratio between electric and magnetic proton form factors was recently analysed in the framework of dispersion relations, using space-like and time-like data [11,12]. However, all the published data in the time-like region [13-16] assumed $G_E = G_M$ to hold for all Q^2 and not only at threshold. Moreover, accurate data at high energy are lacking. Close to threshold the discrepancy between the LEAR [13] and BaBar [16] data has to be resolved. Therefore a measurement of the proton form factors in the time-like region is planned at PANDA at FAIR in proton antiproton annihilation into an electron positron pair with unprecedented high accuracy [17].

As mentioned above, the radiative corrections may be correctly evaluated in the kinematical configuration of the scattering experiment to extract the physics observables of interest. This paper is devoted to a theoretical investigation of the $\bar{p}p \rightarrow e^+e^-$ process including radiative corrections to lowest order of perturbation theory. Among the recent papers devoted to this subject, one should mention [18] where the possibility to measure the charge asymmetry is presented assuming the proton as a point-like particle. The charge-odd part presented in the differential cross section is the

origin of this asymmetry. Recently, the authors of [19] reevaluated this correction in the laboratory frame, omitting the contribution of the hard photon as well as the contribution from the initial state radiation. The first results of full simulations with PANDA detector [17] show that precisions of the order of 3%-5% can be obtained for the cross section measurement. In this context, we need to evaluate the radiative correction due to the final state radiation, namely photon emission from the electron or the positron, as well as the radiation in the initial state at the proton vertex.

In this paper, the complete general radiative corrections to lowest order, to the $\bar{p}p \rightarrow e^+e^-$ channel are investigated, in the kinematical configuration of the planned experiment with the PANDA detector at FAIR. The hard photon contribution from the reaction $\bar{p}p \rightarrow e^+e^-\gamma$ is evaluated with different models assumption for the electromagnetic form factors, in contrast to what was done in [18]. Indeed, to take into account the radiative corrections in the data analysis, we need to know the efficiency and acceptance corrections for a complete simulation. This study is a first step towards a correct extraction of the form factors from angular distribution measurements in the data analysis stage.

2 Electromagnetic nucleon current operator and Born cross section

Let us first introduce our notations and the definition of the electromagnetic nucleon current operator with the magnetic and electric form factors of the nucleon. For the annihilation process, in the one photon exchange approximation:

$$\bar{p}(p^-) + p(p^+) \rightarrow e^+(q^+) + e^-(q^-)$$

The corresponding Feynman diagram for this reaction is given in Fig.1.

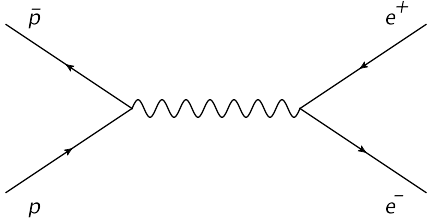


Fig. 1. One photon exchange diagram for the process $\bar{p}p \rightarrow e^+e^-$.

The Born amplitude has the form

$$M^B = \frac{4\pi\alpha}{s} \bar{v}(p^-) \Gamma_\mu u(p^+) \bar{u}(q^-) \gamma^\mu v(q^+) \quad (1)$$

with

$$\Gamma_\mu = F_1(s) \gamma_\mu + \frac{F_2(s)}{4M} [\gamma_\mu, \not{q}] \quad (2)$$

where M is the proton mass and the complex quantities $F_1(s)$ and $F_2(s)$ are the Dirac and Pauli form factors respectively. $G_M(s)$ the magnetic and $G_E(s)$ the electric form factors are related to the Dirac and Pauli form factors F_1 and F_2 by:

$$G_E(s) = F_1(s) + \tau F_2(s) \quad (3)$$

$$G_M(s) = F_1(s) + F_2(s) \quad (4)$$

with

$$s = q^2 = (p^- + p^+)^2, \quad \tau = s/(4M^2) \\ \beta_p^2 = 1 - 4M^2/s$$

The differential cross section in the Born approximation in the center of mass has the form (neglecting the electron mass m):

$$\left[\frac{d\sigma}{d\Omega} \right]_B = \frac{\alpha^2}{4s\beta_p} \{ |G_M(s)|^2 (1 + \cos^2 \theta) \\ + (1 - \beta_p^2) |G_E(s)|^2 \sin^2 \theta \} \quad (5)$$

where θ is the scattering angle of the positron. This cross section was first derived by the authors of [20]. The analytical form is exactly the same for the electron. The expression of the differential cross section in terms of the electric and magnetic form factors shows that we have access only to the modulus of these complex quantities. It is only with a polarized beam or a polarized target that we can learn something on their relative phase. In the particular case, where the proton is considered as a pointlike particle, with $G_M(s) = G_E(s) = 1$, the formula (5) reduces to

$$\left[\frac{d\sigma}{d\Omega} \right]_B^0 = \frac{\alpha^2}{4s\beta_p} \{ 2 - \beta_p^2 \sin^2 \theta \} \quad (6)$$

It should be noted that the shape and the normalization of the differential cross section is sensitive to the model assumption of the form factors. We display in Fig. 2 the distribution for two different models: the "Babar" model -model 1- which is obtained by a fit to the Babar data[16] and the model 2 which is the model of F. Iachello and Q. Wan [21].

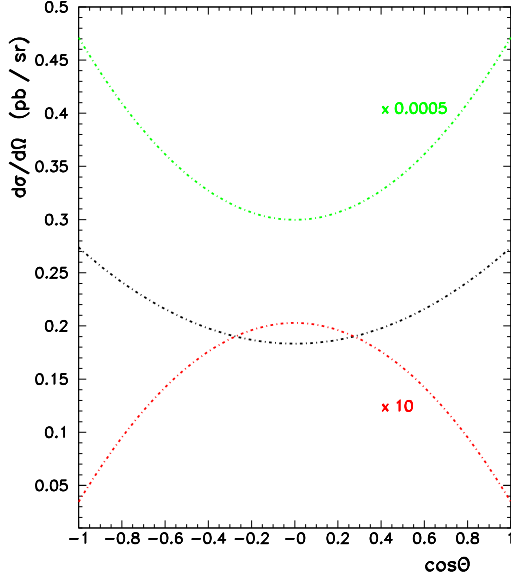


Fig. 2. Born cross section versus $\cos \theta$ for $s = 12.9 \text{ GeV}^2$: point-like model of the proton (green dash-dotted line), model 1 (black dash-dotted line) and model 2 (red line)

For this phenomenological model 1, the form factors G_M and G_E read:

$$G_M = |G_M| e^{i\varphi_M}; \quad G_E = |G_E| e^{i\varphi_E} \quad (7)$$

According to the pQCD asymptotic behavior in the space-like region, the modulus of the magnetic form factor has the form:

$$|G_M| = \frac{A}{q^4 \left(\ln^2 \frac{q^2}{\Lambda_{QCD}^2} + \pi^2 \right)} \quad (8)$$

with

$$\Lambda_{QCD} = 0.3 \text{ GeV} \quad A = 98 \text{ GeV}^4 \quad (9)$$

Another important parameter is the ratio R defined as $R = |G_E| / |G_M|$ which is parametrized by:

$$R = \frac{|G_E|}{|G_M|} = 1 + \left[\frac{q^2}{4M^2} - 0.3 \right]^{-2} \ln \frac{q^2}{4M^2} \quad (10)$$

and the relative phase

$$\varphi_E - \varphi_M = \pi \left[1 - e^{-\frac{1}{2} \left(\frac{q^2}{4M^2} - 1 \right)} \right] \quad (11)$$

The fit to the Babar data are guided by the following constraints:

- 1) $q^2 = 4M^2 \Rightarrow R = 1$
- 2) $q^2 \rightarrow \infty \Rightarrow R \rightarrow 1$
- 3) $q^2 = 4M^2 \Rightarrow \varphi_E - \varphi_M = 0$
- 4) $q^2 \rightarrow \infty \Rightarrow \varphi_E - \varphi_M \rightarrow \pi$

The constraints 1) and 3) follow from the definition of the electric and magnetic form factors in terms of the Dirac F_1 and Pauli F_2 form factors. The constraints 2) and 4) follow from the theorems of Phragmén and Lindelöf [22] which states that the ratio G_E/G_M is the same in both the space-like and the time-like regions when $q^2 \rightarrow \pm\infty$. In the space-like region, these form factors are real and they are asymptotically real also in the time-like region. In the framework of dispersion relations and fitting the available data both in time-like and space-like regions, the authors of ref[11] predict the presence of space-like zero of G_E/G_M at $q^2 = (-11 \pm 2) \text{ GeV}^2$. The fact that the relative phase tends to π radians follows from the relation as mentioned in formula (12) of ref[11] and the presence of the space-like zero ratio.

The shapes of the ratio R versus q^2 for the two models under consideration in this article are displayed in Fig.3.

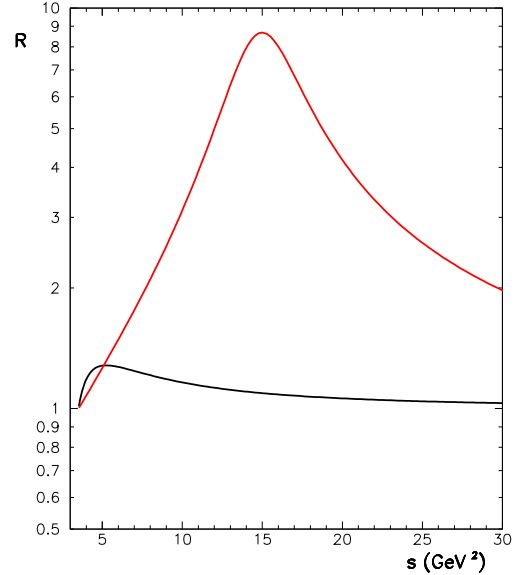


Fig. 3. Ratio R versus s : model 1 (black line) and model 2 (red line)

As it can be seen, the two models are quite different and the final conclusions concerning the effect of the electromagnetic form factors on the radiative corrections should be meaningful.

3 QED Radiative corrections to first order

The proton electromagnetic form factors can be extracted from the angular distribution of the final lepton in the Born cross section. However, this distribution is altered from its zeroth-order shape by radiative corrections. In practice, the distorted distribution by radiative effects can be written as :

$$\left[\frac{d\sigma}{d\Omega} \right]_R = \left[\frac{d\sigma}{d\Omega} \right]_B (1 + \delta) \quad (12)$$

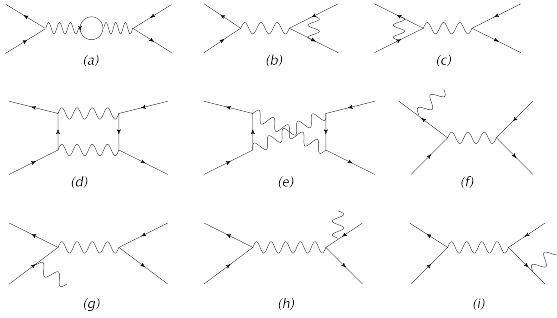


Fig. 4. Feynman diagrams for the first-order radiative correction in $\bar{p}p \rightarrow e^+e^-$.

The set of diagrams contributing to the first order corrections is shown in Fig. 4. The virtual correction comes from the interference between the Born diagram (Fig. 1) and the diagrams (a)-(e) of Fig. 4. The bremsstrahlung from the initial state (diagrams (f) and (g)) alters the effective center of mass energy and significantly changes the kinematics of the final lepton pair. And finally, the photon emission from the final state is represented by the diagrams (h) and (i). Only the bremsstrahlung corrections lead to infrared singularities. These singularities are cancelled order by order by virtual corrections. We adopt the standard treatment of the bremsstrahlung, separating the soft photon contribution with the emitted photon energy up to an infrared cut-off parameter ω where the soft photon approximation holds, and the hard photon contribution from ω up to an experimental cut depending on the energy resolution of the detector. This separation is somewhat arbitrary,

so we have checked that the total radiative correction (Virtual+soft+hard) does not depend on this infrared cut-off.

The virtual and real photon corrections are achieved by the factorization of the cross section in eq.(12) with

$$\delta = \delta_{SV} + \delta_H \quad (13)$$

We write down the soft and virtual correction together to remove the infrared singularities. The remaining term δ_{SV} (soft+virtual) is now finite. The hard photon contribution δ_H depends, of course, on the energy resolution of the detector. The full simulations in a realistic configuration of the detector will allow the determination of the experimental cut on the maximum energy of the real photon emitted or preferably, on the invariant mass spectrum of the final lepton pair.

Below we present the details of our investigation of the different contributions to the radiative corrections in $\bar{p}p \rightarrow e^+e^-$.

3.1 Virtual and soft photon contributions

The detailed expressions of all the terms included in δ_{SV} are given without any kinematical approximation, which allows to use them for any value of the anti-proton kinetic energy and for any angle of the positron.

3.1.1 Virtual correction:

As introduced at the beginning of this section, we have:

$$\left[\frac{d\sigma}{d\Omega} \right]_{BV} = \left[\frac{d\sigma}{d\Omega} \right]_B \{ 1 + \delta_V \} \quad (14)$$

with δ_V , the virtual correction corresponding to the Feynman diagrams (a), (b), (c), (d), (e) of Fig.4 is given by:

$$\delta_V = \delta_{vac} + \delta_{vertex}^e + \delta_{vertex}^p + \delta_{box} \quad (15)$$

For the vacuum polarisation contribution, the loop in diagram (a) of Fig.4 includes the electron loop and the muon-loop [23].

$$\delta_{vac} = \frac{\alpha}{\pi} \left[2 (\Pi_{e^+e^-} + \Pi_{\mu^+\mu^-}) \right] \quad (16)$$

$$\Pi_{e^+e^-} = \frac{1}{3} \left(L_e - \frac{5}{3} \right); \quad L_e = \ln \frac{s}{m^2} \quad (17)$$

$$\Pi_{\mu^+\mu^-} = -\frac{8}{9} + \frac{\beta_\mu^2}{3} + \beta_\mu \left(\frac{1}{2} - \frac{1}{6} \beta_\mu^2 \right) L_\mu \quad (18)$$

$$\beta_\mu = \sqrt{1 - \frac{4M_\mu^2}{s}} \quad L_\mu = \ln \frac{1 + \beta_\mu}{1 - \beta_\mu} \quad (19)$$

where m and M_μ are respectively the electron and the muon mass. The hadronic loop is dominated by the charged pion pair as hadron state. The form factor $F_\pi(s)$, needed in this contribution, will reduce strongly this pion loop contribution. In the energy range of interest ($s > 5 \text{ GeV}^2$) the pion loop term has therefore been removed from the considerations.

At the lepton vertex, the expression of δ_{vertex}^e was derived a long time ago by the authors of [24]. To deal with the infrared divergent term, we consider the extra virtual photon of the process of Fig. 4 with a mass λ .

$$\delta_{vertex}^e = \frac{\alpha}{\pi} \left[2(L_e - 1) - \frac{1}{2} L_e - \frac{1}{2} L_e^2 + \frac{2\pi^2}{3} + 2(1 - L_e) \ln \frac{m}{\lambda} \right] \quad (20)$$

The expressions for δ_{vertex}^p and δ_{box} are derived in the reference [18]. They assume the proton to be a pointlike particle. We give their result in this article for completeness in Appendix A. The validity of the pointlike approximation will be discussed in the next section.

3.1.2 Real photon emission and soft photon contribution

The real photon emission comes from the reaction $\bar{p}p \rightarrow \gamma e^+e^-$. The exact calculation of the cross section of this reaction including the electromagnetic form factors F_1 and F_2 is given in the section 3.2 and in the appendix C.1. The well known infrared singularity, where the energy k_0 of the emitted photon goes to zero, is under control by considering the soft photon contribution. The divergent terms in $\delta_{vertex}^e + \delta_{vertex}^p + \delta_{box}$ have to be cancelled by the divergent parts of the soft photon contributions. In the appendix C.2, we show analytically that the ratio between the soft photon contribution and the Born cross

section is independent of the model used for the form factors.

Within this soft photon approximation, the corrected cross section is related to the Born cross section using (see Appendix C.2)

$$\left[\frac{d\sigma}{d\Omega} \right]_{\text{Soft}} = \left[\frac{d\sigma}{d\Omega} \right]_{\text{B}} \delta_{\text{Soft}} \quad (21)$$

with

$$\delta_{\text{Soft}} = -\frac{\alpha}{2\pi^2} I_{\text{Soft}} \quad (22)$$

and

$$I_{\text{Soft}} = \int_0^{\omega'} \left(\frac{p^+}{k.p^+} - \frac{p^-}{k.p^-} + \frac{q^-}{k.q^-} - \frac{q^+}{k.q^+} \right)^2 \frac{d^3\mathbf{k}}{2k_0} \quad (23)$$

$\omega' = \sqrt{\omega^2 - \lambda^2}$. λ is again the virtual mass of the photon ($\lambda \rightarrow 0$). The term I_{Soft} is expanded as follows:

$$I_{\text{Soft}} = I_{\text{Soft}}^e + I_{\text{Soft}}^p + I_{\text{Soft}}^{\text{ep}} \quad (24)$$

$$I_{\text{Soft}}^e = \int_0^{\omega'} \left(\frac{q^-}{k.q^-} - \frac{q^+}{k.q^+} \right)^2 \frac{d^3\mathbf{k}}{2k_0} \quad (25)$$

gives the contribution of the soft photon emitted by the leptons (diagrams (h) and (i) of Fig.4).

$$I_{\text{Soft}}^p = \int_0^{\omega'} \left(\frac{p^+}{k.p^+} - \frac{p^-}{k.p^-} \right)^2 \frac{d^3\mathbf{k}}{2k_0} \quad (26)$$

is the same quantity for the soft photon emitted by the proton or the antiproton (diagrams (f) and (g) of Fig.4).

$$I_{\text{Soft}}^{\text{ep}} = 2 \int_0^{\omega'} \left(\frac{p^+}{k.p^+} - \frac{p^-}{k.p^-} \right) \left(\frac{q^-}{k.q^-} - \frac{q^+}{k.q^+} \right) \frac{d^3\mathbf{k}}{2k_0} \quad (27)$$

is the contribution of the interference between the initial and final radiation diagrams (diagrams (f)(h); (f)(i); (g)(h); (g)(i) of Fig.4).

The expansion (24) in terms of radiative corrections reads:

$$\delta_{\text{Soft}} = \delta_{\text{Soft}}^e + \delta_{\text{Soft}}^p + \delta_{\text{Soft}}^{\text{ep}} \quad (28)$$

The electron term in the contribution of the soft photon emitted at the lepton vertex can be written as

$$I_{\text{Soft}}^e = m^2 \mathcal{I}_{q^- q^-} + m^2 \mathcal{I}_{q^+ q^+} - 2 q^- \cdot q^+ \frac{\mathcal{L}_{q^- q^+}}{2} \quad (29)$$

with

$$\beta_e^2 = 1 - \frac{4m^2}{s} \quad (30)$$

$$2 q^- \cdot q^+ = s - 2m^2 = \frac{s(1 + \beta_e^2)}{2} \quad (31)$$

Performing the calculation of the two first diagonal terms we get :

$$m^2 \mathcal{I}_{q^- q^-} = m^2 \mathcal{I}_{q^+ q^+} = \pi \left[2 \ln \frac{2\omega}{\lambda} - \ln \frac{s}{m^2} \right] \quad (32)$$

Using our metric à la Bjorken and Drell, the calculation of the non-diagonal term is derived from the 't Hooft and Veltman method [25]. We give more details of this transposition in appendix B.

We need to separate the finite term (finite) from the infrared singularity term (div) depending on λ .

$$\frac{\mathcal{L}_{q^- q^+}(\text{div})}{2} = \frac{2\pi}{s\beta_e} \ln \frac{(1 + \beta_e)^2}{(1 - \beta_e)^2} \ln \frac{2\omega}{\lambda} \quad (33)$$

$$\frac{\mathcal{L}_{q^- q^+}(\text{finite})}{2} = \frac{2\pi}{s\beta_e} \left[Sp\left(-\frac{2\beta_e}{1 - \beta_e}\right) - Sp\left(\frac{2\beta_e}{1 + \beta_e}\right) \right] \quad (34)$$

$$I_{\text{Soft}}^e = -2\pi \left\{ \left[\frac{1 + \beta_e^2}{2\beta_e} \ln \frac{(1 + \beta_e)^2}{(1 - \beta_e)^2} - 2 \right] \ln \frac{2\omega}{\lambda} + \ln \frac{s}{m^2} + \frac{(1 + \beta_e^2)}{2\beta_e} \left[Sp\left(-\frac{2\beta_e}{1 - \beta_e}\right) - Sp\left(\frac{2\beta_e}{1 + \beta_e}\right) \right] \right\} \quad (35)$$

Now for the soft photon emitted at the hadron vertex, I_{Soft}^p is derived from I_{Soft}^e , replacing β_e by β_p :

$$I_{\text{Soft}}^p = -2\pi \left\{ \left[\frac{1 + \beta_p^2}{2\beta_p} \ln \frac{(1 + \beta_p)^2}{(1 - \beta_p)^2} - 2 \right] \ln \frac{2\omega}{\lambda} + \ln \frac{s}{M^2} + \frac{(1 + \beta_p^2)}{2\beta_p} \left[Sp\left(-\frac{2\beta_p}{1 - \beta_p}\right) - Sp\left(\frac{2\beta_p}{1 + \beta_p}\right) \right] \right\} \quad (36)$$

Here again, we separate the interference term between the soft photon contribution from the lepton and hadron vertex into an infrared divergent term depending on the mass λ and a finite term:

$$I_{\text{Soft}}^{\text{ep}}(\text{div}) = 4\pi \ln \frac{M^2 - t}{M^2 - u} \ln \frac{M^2}{\lambda^2} \quad (37)$$

$$I_{\text{Soft}}^{\text{ep}}(\text{finite}) = 4\pi \left\{ 2 \ln \frac{M^2 - t}{M^2 - u} \ln \frac{2\omega}{M} + Sp\left(1 + \frac{(1 + \beta_p)st}{2M^4}\right) - Sp\left(1 + \frac{(1 + \beta_p)su}{2M^4}\right) + Sp\left(1 + \frac{st}{(M^2 - t)^2}\right) - Sp\left(1 + \frac{su}{(M^2 - u)^2}\right) + Sp\left(1 + \frac{(1 - \beta_p)st}{2M^4}\right) - Sp\left(1 + \frac{(1 - \beta_p)su}{2M^4}\right) \right\} \quad (38)$$

In eqs.(34-38), $Sp(x)$ is the dilogarithm or Spence's function defined as :

$$Sp(x) = - \int_0^x \frac{\ln(1 - t)}{t} dt$$

One can check that the infrared terms depending on λ disappear when we sum up the contributions from the virtual and soft photon corrections.

We show in the table 1 and in the table 2, the soft and virtual corrections with final and initial state radiations as a function of the positron angle in the center of mass system. The left columns represent the individual contributions δ_{vac} , δ_{vertex}^e and δ_{Soft}^e which are usually calculated. The other contributions are δ_{vertex}^p , δ_{Soft}^p , δ_{box} and the interference contribution $\delta_{\text{Soft}}^{\text{ep}}$ of the emitted soft photons. The right columns give the quantities

$$\delta_{SV}^e = \delta_{vac} + \delta_{vertex}^e + \delta_{\text{Soft}}^e$$

and the total contribution

$$\delta_{SV}^{ep} = \delta_{SV}^e + \delta_{vertex}^p + \delta_{Soft}^p + \delta_{box} + \delta_{Soft}^{ep}$$

The upper limit of the energy of the soft photon, separating the soft and hard photon contributions is denoted by ω . Its value has been chosen such as the ratio of this energy to the energy of the positron in the center of mass, when no photon is emitted, is $\simeq 1\%$.

Let us add some comments on the radiative correction (soft+virtual) factor values in the two last columns of tables 1,2.

- If only the final state radiation is taken into account, it is independent of the lepton scattering angle in the center of mass system. This is not the case for the initial state radiation, due mainly to the interference between the initial and final state radiations given by δ_{Soft}^{ep} .
- A remarkable feature is the asymmetry observed in the lepton angular distribution due to the charge-odd term. The angular distributions of the e^+ and e^- are different.
- The contribution of the box diagrams (two-photon exchange) is found to be negligible, less than 1 %. Recently, two-photon corrections in the $\bar{p}p \rightarrow e^+e^-$ process were investigated with the hard rescattering mechanism [26]. To be valid, the virtualities of both photons must be large in such an approach. The two-photon correction obtained is below the 1 % level.
- The contribution of the box diagrams and the proton vertex, which depend on the electromagnetic form factors F_1 and F_2 have only been calculated in [18] in the point-like approximation. As their contribution is small compared to the sum of all the terms, we conclude that this approximation is nevertheless good enough to give a reliable evaluation of the radiative corrections.

As we will see, the hard photon contributions in the next section do not alter these features.

3.2 Hard photon emission

We consider next the contribution from hard photon emission :

$$\bar{p}(p^-) + p(p^+) \rightarrow e^+(q^+) + e^-(q^-) + \gamma(k)$$

The invariant mass W of the (e^+e^-) system is defined by:

$$W^2 = (q^+ + q^-)^2 = (p^- + p^+ - k)^2$$

The models of the proton form factors -model 1 and model 2 - are introduced in our calculation of the hard photon contribution.

The amplitude is written as a sum of four amplitudes :

$$\mathcal{M} = \mathcal{M}_1 + \mathcal{M}_2 + \mathcal{M}_3 + \mathcal{M}_4 \quad (39)$$

$\mathcal{M}_1, \mathcal{M}_2, \mathcal{M}_3, \mathcal{M}_4$ are respectively the amplitudes of the diagrams (h), (i), (f), (g) of Fig. 4. The amplitude \mathcal{M} is written as:

$$\mathcal{M}(\lambda, \lambda_{e^+}, \lambda_{e^-}; \lambda_{\bar{p}}, \lambda_p) = \sum_i \frac{A_i^\sigma(\lambda_{e^+}, \lambda_{e^-}; \lambda_{\bar{p}}, \lambda_p)}{D_i} \varepsilon_\sigma^*(k, \lambda) \quad (40)$$

where $\varepsilon_\sigma^*(k, \lambda)$ is the polarisation vector of the emitted photon with the helicity λ and $\lambda_{e^+}, \lambda_{e^-}, \lambda_{\bar{p}}$ and λ_p are respectively the spin components of the positron, the electron, the proton and the antiproton.

The expressions of $A_i^\sigma(\lambda_{e^+}, \lambda_{e^-}; \lambda_{\bar{p}}, \lambda_p)$ and D_i are given in Appendix C. The sum over the photon helicity in $|\mathcal{M}|^2$ is given by

$$\begin{aligned} & \sum_\lambda |\mathcal{M}(\lambda, \lambda_{e^+}, \lambda_{e^-}; \lambda_{\bar{p}}, \lambda_p)|^2 \\ &= \sum_{ij=1}^4 \frac{A_i^\sigma(\lambda_{e^+}, \lambda_{e^-}; \lambda_{\bar{p}}, \lambda_p) A_j^{\sigma'*}(\lambda_{e^+}, \lambda_{e^-}; \lambda_{\bar{p}}, \lambda_p)}{D_i D_j} \\ & \quad \sum_\lambda \varepsilon_\sigma^*(k, \lambda) \varepsilon_{\sigma'}(k, \lambda) \\ &= - \sum_{ij=1}^4 \frac{A_i^\sigma(\lambda_{e^+}, \lambda_{e^-}; \lambda_{\bar{p}}, \lambda_p) A_{\sigma j}^*(\lambda_{e^+}, \lambda_{e^-}; \lambda_{\bar{p}}, \lambda_p)}{D_i D_j} \end{aligned} \quad (41)$$

We define the X_{ij} quantity by:

$$\begin{aligned} X_{ij} &= \\ &= - \sum_{\lambda_f} A_i^\sigma(\lambda_{e^+}, \lambda_{e^-}; \lambda_{\bar{p}}, \lambda_p) A_{\sigma j}^*(\lambda_{e^+}, \lambda_{e^-}; \lambda_{\bar{p}}, \lambda_p) \end{aligned} \quad (42)$$

where the sum over λ_f means that the sum is performed over all different fermion spin components $\lambda_{e^+}, \lambda_{e^-}, \lambda_{\bar{p}}, \lambda_p$. Because of the fast variation of the propagators with the angle of the emitted photon, it is convenient to write the sum over the spins as follows:

$$\sum_{\lambda, \lambda_f} |\mathcal{M}(\lambda, \lambda_{e^+}, \lambda_{e^-}; \lambda_{\bar{p}}, \lambda_p)|^2 = \sum_{ij} \frac{X_{ij}}{D_i D_j} \quad (43)$$

In total, we have ten different terms:

$$\begin{aligned} \sum_{\lambda, \lambda_f} |\mathcal{M}(\lambda, \lambda_f)|^2 = & \frac{X_{11}}{D_1^2} + \frac{X_{22}}{D_2^2} + \frac{X_{33}}{D_3^2} + \frac{X_{44}}{D_4^2} + \frac{X_{12} + X_{21}}{D_1 D_2} \\ & + \frac{X_{13} + X_{31}}{D_1 D_3} + \frac{X_{14} + X_{41}}{D_1 D_4} + \frac{X_{23} + X_{32}}{D_2 D_3} \\ & + \frac{X_{24} + X_{42}}{D_2 D_4} + \frac{X_{34} + X_{43}}{D_3 D_4} \end{aligned} \quad (44)$$

The expressions of these terms X_{ij} are written out in Appendix C.

The differential cross section in the center of mass system is given by:

$$\begin{aligned} \frac{d^5\sigma}{dE_\gamma d\Omega_\gamma d\Omega_{e^+}} = & \frac{(\hbar c)^2}{32(2\pi)^5} \frac{1}{|\mathbf{p}^-|} \frac{1}{\sqrt{s}} \frac{1}{4} \\ & \sum_{\lambda, \lambda_f} J_{ac} E_\gamma |\mathcal{M}(\lambda, \lambda_{e^+}, \lambda_{e^-}; \lambda_{\bar{p}}, \lambda_p)|^2 \end{aligned} \quad (45)$$

where the jacobian J_{ac} is equal to:

$$J_{ac} = \frac{|\mathbf{q}^+|^3}{|\mathbf{q}^+|^2 E_{e^-} + E_{e^+} (|\mathbf{q}^+|^2 + \mathbf{k} \cdot \mathbf{q}^+)} \quad (46)$$

This differential cross section can then be expressed as:

$$\frac{d^5\sigma}{dE_\gamma d\Omega_\gamma d\Omega_{e^+}} = \sum_{1 \leq i, j \leq 4} \left[\frac{d^5\sigma}{dE_\gamma d\Omega_\gamma d\Omega_{e^+}} \right]_{ij} \quad (47)$$

4 Total Radiative corrections and Numerical Results.

In this section, we study the radiative corrections which have to be applied to the e^+e^- invariant mass spectrum. These corrections depend of the experimental cut W_{max} . In the center of mass, the relation between this invariant mass and the photon energy is simple:

$$s - 2E_\gamma \sqrt{s} = W^2 \quad (48)$$

We split the cross section in a virtual+soft part and a hard photon part as:

$$\begin{aligned} \left[\frac{d^2\sigma}{d\Omega_{e^+}} \right]_R (E_\gamma^{max}) = & \left[\frac{d^2\sigma}{d\Omega_{e^+}} \right]_B (1 + \delta_{SV}(\omega)) \\ & + \int_\omega^{E_\gamma^{max}} \frac{d^5\sigma}{dE_\gamma d\Omega_\gamma d\Omega_{e^+}} dE_\gamma d\Omega_\gamma \end{aligned} \quad (49)$$

We expect the cross section given by eq.(49) to be practically independent of the cut-off ω .

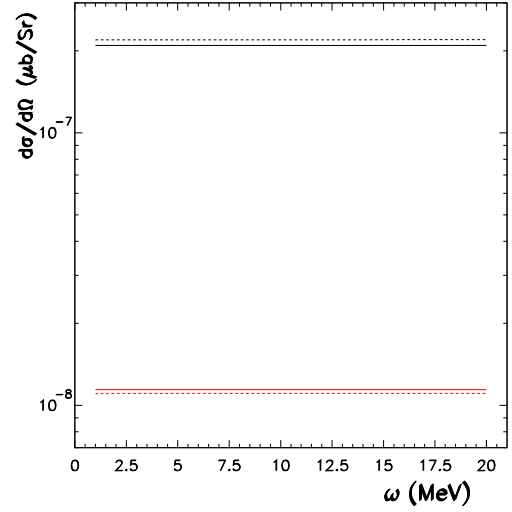


Fig. 5. Corrected cross section versus the infrared cut-off parameter ω for $s = 12.9 \text{ GeV}^2$ and $\theta_{e^+} = 45^\circ$: (model 1 : black line and model 2 : red line). The dotted lines correspond to the situation where only the final state contribution is included.

It is indeed what we see on fig.5, with a calculation at $\theta_{e^+} = 45^\circ$ and up to a photon energy E_γ^{max} of 0.4 GeV. In this calculation, the variation of ω is $1/1000 \leq \omega/E_{e^+} \leq 1/100$. Within this variation of ω , we do not see any difference in the stability with the photons emitted by the leptons alone or by the leptons and the hadrons. Furthermore, there is no effect due to the model. The same conclusions hold for $s = 5.4 \text{ GeV}^2$.

The correction factor δ_H is the ratio between the cross section with an extra real photon and the Born cross section, with the electromagnetic factors included and without the soft photon approximation. Looking at the expression (48), it is alluring to define the quantities δ^e and δ^{ep} as:

$$\delta^e = \delta_{SV}^e(\omega) + \sum_{1 \leq i,j \leq 2} \mathcal{R}_{ij} \quad (50)$$

$$\delta^{ep} = \delta_{SV}^{ep}(\omega) + \sum_{1 \leq i,j \leq 4} \mathcal{R}_{ij} \quad (51)$$

with

$$\mathcal{R}_{ij} = \int_{\omega}^{E_{\gamma}^{max}} \left[\frac{d^5\sigma}{dE_{\gamma} d\Omega_{\gamma} d\Omega_{e^+}} \right]_{ij} dE_{\gamma} d\Omega_{\gamma} / \left[\frac{d^2\sigma}{d\Omega_{e^+}} \right]_B \quad (52)$$

We now give the numerical results associated with these formula. The variation of the cross section as a function of the invariant mass square of the (e^+e^-) system is shown in Fig. 6.

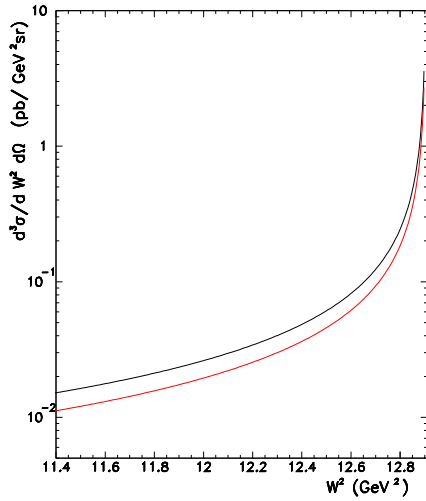


Fig. 6. (Color online) Differential cross section $d^2\sigma/dW^2 d\Omega_{e^+}$ as a function of W^2 (W is the invariant mass of the (e^+e^-) system), for $s = 12.9 \text{ GeV}^2$, $E_{\gamma}^{max} = 100 \text{ MeV}$ and $\theta_{e^+} = 30^\circ$ (model 1 : black line and model 2 : red line)

The numerical results strongly depend on the experimental energy cut-off of the emitted photon. We have chosen to give in this article the results for a cut-off energy E_{γ}^{max} of 0.1 GeV. The values of the

δ parameters for some positron angles are given in Table 3 using model 2.

Table 3. Total radiative corrections for $s = 5.4 \text{ GeV}^2$ (two left columns) and for $s = 12.9 \text{ GeV}^2$ (two right columns), assuming the energy of the hard photon emission up to 100 MeV

	$s = 5.4 \text{ GeV}^2$		$s = 12.9 \text{ GeV}^2$	
$\theta_{e^+} (\text{deg.})$	δ^e	δ^{ep}	δ^e	δ^{ep}
30.	-0.0952	-0.1300	-0.1320	-0.2191
60.	-0.0952	-0.1096	-0.1320	-0.1783
90.	-0.0952	-0.0878	-0.1320	-0.1419
120.	-0.0952	-0.0629	-0.1320	-0.0986
150.	-0.0952	-0.0396	-0.1320	-0.0528

The dependence of the radiative correction with the positron angle is displayed in Figs. 7-8.

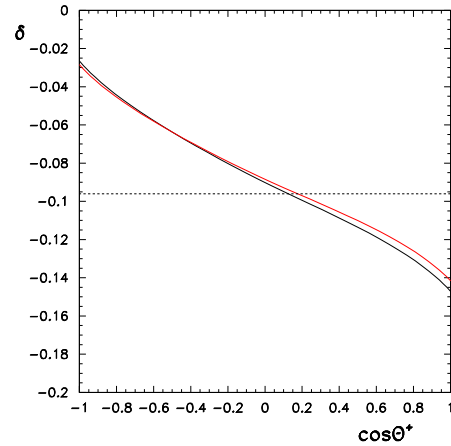


Fig. 7. (Color online) Total radiative correction δ as a function of $\cos \theta_{e^+}$ in the CM frame for $s = 5.4 \text{ GeV}^2$ and $E_{\gamma}^{max} = 100 \text{ MeV}$ (model 1 : black line and model 2 : red line). The dashed line corresponds to the situation where only the final state radiation contributes.

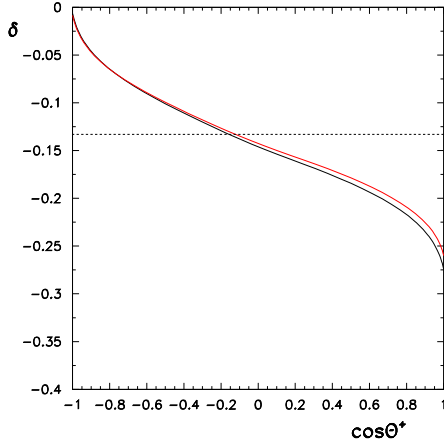


Fig. 8. (Color online) Total radiative corrections factor δ as a function of $\cos \theta_{e^+}$ in the CM frame for $s = 12.9 \text{ GeV}^2$ and $E_{\gamma}^{max} = 100 \text{ MeV}$ (model 1 : black line and model 2 : red line). The dashed line corresponds to the situation where only the final state radiation contributes.

If only the final state radiation contributes, the value of δ is independent of the positron angle in the C.M. system. In contrast, when the initial and final state radiations are taken into account, we notice large differences in the value of the correction factor δ at backward and forward positron angles (Figs:7,8). The main reason for this effect is the interference term. Let us emphasize the practically independent correction factor δ with the model used for the electromagnetic form factors.

The corrected cross section is displayed for comparison with the Born cross section in Fig. 9. The different curves are obtained using the model 1 for the form factors. Of course the normalisation of these cross sections depend on the model assumptions. One can also remark the asymmetry of the black line due to the charge-odd term when the initial state radiation at the hadron vertex is included. The measurement of this asymmetry term included in the angular distribution seems to be a difficult task.

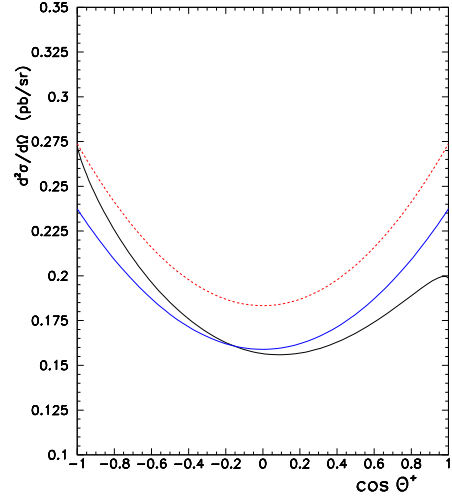


Fig. 9. (Color online) Corrected differential cross section $d^2\sigma/d\Omega_{e^+}$ as a function of $\cos \theta_{e^+}$ in the CM frame, for $s = 12.9 \text{ GeV}^2$, $E_{\gamma}^{max} = 100 \text{ MeV}$ (black line). The corresponding blue line corresponds to the situation where only the final state radiation contributes. The red dotted line is the Born cross section with the assumption model 1 for the form factors.

The total radiative correction have an important symmetry that is worth to mention. The values of δ are the corrections to the angular distribution of the positron (e^+). The corresponding distribution of the electron (e^-) is obtained by replacing (θ) by $(\pi - \theta)$ in order to respect the C-charge symmetry. We have checked numerically that the total radiative correction reads :

$$\delta^{(e^+)}(\theta) = \delta^{(e^-)}(\pi - \theta)$$

This observation led us to define two interesting observables namely:

$$\mathcal{S} = \frac{1}{2} \left(\frac{d\sigma}{d\Omega_{e^+}} + \frac{d\sigma}{d\Omega_{e^-}} \right) \quad (53)$$

and

$$\mathcal{A} = \left(\frac{d\sigma}{d\Omega_{e^+}} - \frac{d\sigma}{d\Omega_{e^-}} \right) \bigg/ \left(\frac{d\sigma}{d\Omega_{e^+}} + \frac{d\sigma}{d\Omega_{e^-}} \right) \quad (54)$$

The first one contains the charge-even terms and is the corrected Born cross section for form factors extraction. For this observable, we have

$$\frac{d\sigma}{d\Omega_e} = \left[\frac{d\sigma}{d\Omega_e} \right]_B (1 + \delta^S) \quad (55)$$

with

$$\delta^S = \frac{1}{2} [\delta(\theta) + \delta(\pi - \theta)] \quad (56)$$

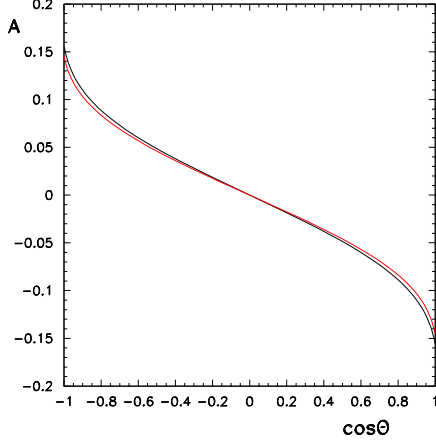


Fig. 10. (Color online) Asymmetry \mathcal{A} versus $\cos\theta$ for $s = 12.9 \text{ GeV}^2$; for $E_{\gamma}^{max} = 100 \text{ MeV}$ (model 1 : black line and model 2 : red line)

The second one is the charge asymmetry observable due to the odd part. The value of this charge asymmetry term \mathcal{A} is rather large and can be measured with the PANDA detector (Fig. 10). The shape and the normalization of the observable \mathcal{S} is model-dependent and could be used to discriminate between different models of the form factors.

5 Conclusions

We conclude that the initial state radiation (at the hadron vertex) is not negligible and can be calculated and incorporated into the total radiative correction. If the precision of the cross section measurement is of the order of 3-5%, the total model independent correction obtained in this paper can be used to correct the measured cross section, before the comparison with the Born cross section needed to discriminate between the different model assumptions of the proton form factors.

We have shown that the interference between the initial and final state radiations is the main contribution to the charge asymmetry \mathcal{A} . The evaluation of this radiative correction in terms of structure functions and evolution equations [27] must be performed

with caution. A study of the angular distribution of the photon shows a non negligible part of the photons emitted outside the cone of angle $\theta_{\gamma} \leq m/E$.

In contrast to space-like elastic electron-proton scattering, in the time-like region we can consider the shape of the e^+ and e^- angular distributions separately to exhibit the charge asymmetry. The numerical result displayed in Fig. 9 shows the limit of this statement. We suggest the measurement of two observables namely \mathcal{S} and \mathcal{A} .

With the PANDA detector, an accurate calculation of the differential cross section of the lepton pair and of the real photon is needed to disentangle the $\bar{p}p \rightarrow (\gamma)e^+e^-$ reaction from the $\bar{p}p \rightarrow \pi^+ \pi^-$ reaction. As the pion counting rate is huge compared to the lepton counting rate, the angular distribution of the real photon has to be known as precisely as possible, so the photon emission in the proton anti-proton side can not be ignored. Based on the formalism described in this article, we have developed a Monte Carlo Code. A full simulation is needed to take into account the radiative corrections together with efficiency and acceptance corrections. Based on the Babar data, the model 1 for the electromagnetic form factors allows to have a realistic calculation of the $\bar{p}p \rightarrow (\gamma)e^+e^-$ process. Contrary to the model 2 and the point-like model, it gives the good order of magnitude of the counting rate.

6 Acknowledgments

The authors would like to thank the ORSAY/PANDA Collaboration members for constructive remarks and constant encouragements, in particular R. Kunne for a careful reading of the manuscript.

A Proton vertex and Box diagrams contribution

The derivation given in this appendix is due to the work of the authors of ref[18].

For δ_{vertex}^p corresponding to the Feynman graph (c) of Fig. 4, the correction is given by:

$$\delta_{vertex}^p = \frac{\alpha}{\pi} F_{vertex}^p \quad (57)$$

where F_{vertex}^p is the sum of two terms.:

$$F_{vertex}^p = 2F_1^{(2)} + \frac{4F_2^{(2)}}{2 - \beta_p^2 \sin^2 \theta} \quad (58)$$

The first one contains the infrared divergence:

$$F_1^{(2)} = -1 - \frac{1}{4\beta_p} L_{\beta_p} + \frac{1+\beta_p^2}{2\beta_p} \left[\frac{\pi^2}{3} + L_{\beta_p} + Sp\left(\frac{1-\beta_p}{1+\beta_p}\right) - \frac{1}{4} L_{\beta_p}^2 - L_{\beta_p} \ln \frac{2\beta_p}{1+\beta_p} \right] + \left(1 - \frac{1+\beta_p^2}{2\beta_p} L_{\beta_p}\right) \ln \frac{M}{\lambda} \quad (59)$$

while the second term is finite:

$$\frac{4F_2^{(2)}}{2-\beta_p^2 \sin^2 \theta} = -\frac{1-\beta_p^2}{\beta_p} \frac{L_{\beta_p}}{2-\beta_p^2 \sin^2 \theta} \quad (60)$$

$$L_{\beta_p} = \ln \frac{1+\beta_p}{1-\beta_p} \quad (61)$$

To give the formulas related to the box diagrams contribution, we first remind the reader the usual expressions for the Mandelstam variables s , t and u of the process namely

$$s = (p^- + p^+)^2, \quad t = (p^- - q^+)^2, \quad u = (p^- - q^-)^2$$

The two-photon correction is given by:

$$\delta_{box} = \frac{\alpha}{\pi} \frac{s I(s, t, u)}{\Delta} \quad (62)$$

with

$$\Delta = t^2 + u^2 - 4M^2(t+u) + 6M^4 \quad (63)$$

The quantity $I(s, t, u)$ (Eq.(20) of Ref.[18]) is the sum of five terms:

$$I(s, t, u) = \sum_{i=1}^5 I^i(s, t, u) \quad (64)$$

The infrared divergence is contained in the last term:

$$\frac{s I^5(s, t, u)}{\Delta} = 2 L_{tu} L_{M\lambda} + 2 L_{tu} L_s \quad (65)$$

Following eq.(64), we have

$$\delta_{box} = \sum_{i=1}^5 \delta_{i \text{ box}} \quad (66)$$

$$\delta_{1 \text{ box}} = \frac{\alpha}{\pi} \frac{s(u-t)}{\Delta} \left[\left(\frac{2M^2}{\beta_p^2} + t + u \right) I_0 - \frac{\pi^2}{6} + \frac{1}{2} L_{\beta_p}^2 - \frac{L_{\beta_p}}{\beta_p^2} \right] \quad (67)$$

with

$$I_0 = \frac{1}{s\beta_p} \left\{ L_s L_{\beta_p} - \frac{1}{2} L_{\beta_p}^2 - \frac{\pi^2}{6} + 2Sp\left(\frac{1+\beta_p}{2}\right) - 2Sp\left(\frac{1-\beta_p}{2}\right) - 2Sp\left(-\frac{1-\beta_p}{1+\beta_p}\right) \right\} \quad (68)$$

and

$$\delta_{2 \text{ box}} = \frac{\alpha}{\pi} \frac{s(2t+s)}{\Delta} \left[\frac{1}{2} L_{ts}^2 - Sp\left(\frac{-t}{M^2-t}\right) \right] \quad (69)$$

$$\delta_{3 \text{ box}} = -\frac{\alpha}{\pi} \frac{s(2u+s)}{\Delta} \left[\frac{1}{2} L_{us}^2 - Sp\left(\frac{-u}{M^2-u}\right) \right] \quad (70)$$

$$\delta_{4 \text{ box}} = \frac{\alpha}{\pi} \frac{s(ut - M^2(s+M^2))}{\Delta} \left[\frac{L_{ts}}{t} - \frac{L_{us}}{u} + \frac{u-t}{ut} L_s \right] \quad (71)$$

$$\delta_{5 \text{ box}} = \frac{\alpha}{\pi} (2 L_{tu} L_s + 2 L_{tu} L_{M\lambda}) \quad (72)$$

$$L_s = \ln \frac{s}{M^2} \quad L_{tu} = \ln \frac{M^2-t}{M^2-u} \quad (73)$$

$$L_{ts} = \ln \frac{M^2-t}{s} \quad L_{us} = \ln \frac{M^2-u}{s} \quad (74)$$

$$L_{\beta_p} = \ln \frac{1+\beta_p}{1-\beta_p} \quad L_{M\lambda} = \ln \frac{M^2}{\lambda^2} \quad (75)$$

B 't Hooft and Veltman integrals

We need to calculate the integral of the type :

$$\frac{\mathcal{L}_{ij}}{2} = \int_0^{\omega'} \frac{1}{(p_i \cdot k)(p_j \cdot k)} \frac{d^3 \mathbf{k}}{2k_0} \quad (76)$$

where $\omega' = \sqrt{\omega^2 - \lambda^2}$ and $\omega = (k_0)_{max}$ is the maximum energy of the soft photon.

$$p = \eta p_i \quad q = p_j \quad (p - q)^2 = 0 \quad (77)$$

$$\eta^2 p_i^2 - 2\eta p_i \cdot p_j + p_j^2 = 0 \quad (78)$$

$$\ell = p_0 - q_0 \quad v = \frac{p^2 - q^2}{2\ell} \quad (79)$$

with the condition that $(\eta p_i - p_j)_0$ and p_{j0} have the same sign.

The integral \mathcal{L}_{ij} is the sum of a divergent part and a finite part. Using Spence's function rather than its approximation, we get:

$$\mathcal{L}_{ij}(\text{div}) = 2\pi \frac{\eta}{v\ell} \ln \frac{p^2}{q^2} \ln \frac{2\omega}{\lambda} \quad (80)$$

$$\mathcal{L}_{ij}(\text{finite}) =$$

$$\begin{aligned} & 2\pi \frac{\eta}{v\ell} \left[\frac{1}{4} \ln^2 \frac{p_0 - |\mathbf{p}|}{p_0 + |\mathbf{p}|} - \frac{1}{4} \ln^2 \frac{q_0 - |\mathbf{q}|}{q_0 + |\mathbf{q}|} \right] \\ & + 2\pi \frac{\eta}{v\ell} \left[Sp\left(1 - \frac{p_0 + |\mathbf{p}|}{v}\right) - Sp\left(1 - \frac{q_0 + |\mathbf{q}|}{v}\right) \right] \\ & + 2\pi \frac{\eta}{v\ell} \left[Sp\left(1 - \frac{p_0 - |\mathbf{p}|}{v}\right) - Sp\left(1 - \frac{q_0 - |\mathbf{q}|}{v}\right) \right] \end{aligned} \quad (81)$$

C Real photon emission.

C.1 Hard photon contribution.

C.1.1 Amplitudes.

Defining

$$\Gamma_{NN\gamma}^\sigma(k) = F_{10}(k^2)\gamma^\sigma - \frac{F_{20}(k^2)}{4M}(\not{k}\gamma^\sigma - \gamma^\sigma \not{k}) \quad (82)$$

$$F_{10}(k^2) = 1 \quad F_{20}(k^2) = \kappa_p \quad (83)$$

where κ_p is the anomalous magnetic moment of the proton and

$$q' = p^- + p^+ - k = q - k \quad (84)$$

$$\mathcal{M}_i(\lambda, \lambda_{e^+}, \lambda_{e^-}; \lambda_{\bar{p}}, \lambda_p) =$$

$$\frac{A_i^\sigma(\lambda_{e^+}, \lambda_{e^-}; \lambda_{\bar{p}}, \lambda_p)}{D_i} \varepsilon_\sigma^*(k, \lambda) \quad i = 1, 4 \quad (85)$$

$$A_1^\sigma(\lambda_{e^+}, \lambda_{e^-}; \lambda_{\bar{p}}, \lambda_p) = \frac{i}{q^2} e_p e_{e^-}^2$$

$$\left[\bar{v}_{\bar{p}} \Gamma_{NN\gamma}^\mu(q) u_p \right] \left[\bar{u}_{e^-} \gamma_\mu (-\not{k} - \not{q}^+ + m) \gamma^\sigma v_{e^+} \right] \quad (86)$$

$$D_1 = (k + q^+)^2 - m^2 = 2k \cdot q^+ \quad (87)$$

$$A_2^\sigma(\lambda_{e^+}, \lambda_{e^-}; \lambda_{\bar{p}}, \lambda_p) = \frac{i}{q^2} e_p e_{e^-}^2$$

$$\left[\bar{v}_{\bar{p}} \Gamma_{NN\gamma}^\mu(q) u_p \right] \left[\bar{u}_{e^-} \gamma^\sigma (\not{k} + \not{q}^- + m) \gamma_\mu v_{e^+} \right] \quad (88)$$

$$D_2 = (k + q^-)^2 - m^2 = 2k \cdot q^- \quad (89)$$

$$A_3^\sigma(\lambda_{e^+}, \lambda_{e^-}; \lambda_{\bar{p}}, \lambda_p) = \frac{i}{q'^2} e_p^2 e_{e^-}$$

$$\left[\bar{v}_{\bar{p}} \Gamma_{NN\gamma}^\sigma(k) (\not{k} - \not{p}^- + M) \Gamma_{NN\gamma}^\mu(q') u_p \right] \left[\bar{u}_{e^-} \gamma_\mu v_{e^+} \right] \quad (90)$$

$$D_3 = (p^- - k)^2 - M^2 = -2k \cdot p^- \quad (91)$$

$$A_4^\sigma(\lambda_{e^+}, \lambda_{e^-}; \lambda_{\bar{p}}, \lambda_p) = \frac{i}{q'^2} e_p^2 e_{e^-}$$

$$\left[\bar{v}_{\bar{p}} \Gamma_{NN\gamma}^\mu(q') (\not{p}^+ - \not{k} + M) \Gamma_{NN\gamma}^\sigma(k) u_p \right] \left[\bar{u}_{e^-} \gamma_\mu v_{e^+} \right] \quad (92)$$

$$D_4 = (p^+ - k)^2 - M^2 = -2k \cdot p^+ \quad (93)$$

C.1.2 Cross section.

We define:

$$\bar{T}_{NN\gamma}^\nu(x) = F_1^*(x^2)\gamma^\nu - \frac{F_2^*(x^2)}{4M}(\gamma^\nu \not{x} - \not{x}\gamma^\nu) \quad (94)$$

$$\bar{T}_{NN\gamma}^\sigma(k) = F_{10}(k^2)\gamma^\sigma - \frac{F_{20}(k^2)}{4M}(\gamma^\sigma \not{k} - \not{k}\gamma^\sigma) \quad (95)$$

$$\not{p}_M^- = \not{p}^- - M \quad \not{p}_M^+ = \not{p}^+ + M \quad (96)$$

$$\not{q}_m^- = \not{q}^- + m \quad \not{q}_m^+ = \not{q}^+ - m \quad (97)$$

Each X_{ij} term is the product of a constant times Y_{ij} , the product of a hadronic tensor by a leptonic tensor. Each tensor is equal to the trace of linear combination of the product of Dirac matrices:

$$X_{11} = -\frac{e_p^2 e_e^4}{q^4} \text{Tr} \left\{ \not{p}_M^- \Gamma_{NN\gamma}^\mu(q) \not{p}_M^+ \bar{\Gamma}_{NN\gamma}^\nu(q) \right\} \\ \text{Tr} \left\{ \not{q}_m^- \gamma_\mu (-\not{k} - \not{q}_m^+) \gamma^\sigma \not{q}_m^+ \gamma_\sigma (-\not{k} - \not{q}_m^+) \gamma_\nu \right\} \quad (98)$$

$$X_{12} = -\frac{e_p^2 e_e^4}{q^4} \text{Tr} \left\{ \not{p}_M^- \Gamma_{NN\gamma}^\mu(q) \not{p}_M^+ \bar{\Gamma}_{NN\gamma}^\nu(q) \right\} \\ \text{Tr} \left\{ \not{q}_m^- \gamma_\mu (-\not{k} - \not{q}_m^+) \gamma^\sigma (\not{q}^+ - m) \gamma_\nu (\not{k} + \not{q}_m^-) \gamma_\sigma \right\} \quad (99)$$

$$X_{21} = -\frac{e_p^2 e_e^4}{q^4} \text{Tr} \left\{ \not{p}_M^- \Gamma_{NN\gamma}^\mu(q) \not{p}_M^+ \bar{\Gamma}_{NN\gamma}^\nu(q) \right\} \\ \text{Tr} \left\{ \not{q}_m^- \gamma^\sigma (\not{k} + \not{q}_m^-) \gamma_\mu \not{q}_m^+ \gamma_\sigma (-\not{k} - \not{q}_m^+) \gamma_\nu \right\} \quad (100)$$

$$X_{22} = -\frac{e_p^2 e_e^4}{q^4} \text{Tr} \left\{ \not{p}_M^- \Gamma_{NN\gamma}^\mu(q) \not{p}_M^+ \bar{\Gamma}_{NN\gamma}^\nu(q) \right\} \\ \text{Tr} \left\{ \not{q}_m^- \gamma^\sigma (\not{k} + \not{q}_m^-) \gamma_\mu \not{q}_m^+ \gamma_\nu (\not{k} + \not{q}_m^-) \gamma_\sigma \right\} \quad (101)$$

$$X_{13} = -\frac{e_p^3 e_e^3}{q^2 q'^2} \text{Tr} \left\{ \not{q}_m^- \gamma_\mu (-\not{k} - \not{q}_m^+) \gamma_\sigma \not{q}_m^+ \gamma_\nu \right\} \\ \text{Tr} \left\{ \not{p}_M^- \Gamma_{NN\gamma}^\mu(q) \not{p}_M^+ \bar{\Gamma}_{NN\gamma}^\nu(q') (\not{k} - \not{p}_M^-) \bar{\Gamma}_{NN\gamma}^\sigma(k) \right\} \quad (102)$$

$$X_{14} = -\frac{e_p^3 e_e^3}{q^2 q'^2} \text{Tr} \left\{ \not{q}_m^- \gamma_\mu (-\not{k} - \not{q}_m^+) \gamma_\sigma \not{q}_m^+ \gamma_\nu \right\} \\ \text{Tr} \left\{ \not{p}_M^- \Gamma_{NN\gamma}^\mu(q) \not{p}_M^+ \bar{\Gamma}_{NN\gamma}^\sigma(k) (\not{p}_M^+ - \not{k}) \bar{\Gamma}_{NN\gamma}^\nu(q') \right\} \quad (103)$$

$$X_{23} = -\frac{e_p^3 e_e^3}{q^2 q'^2} \text{Tr} \left\{ \not{q}_m^- \gamma_\sigma (\not{k} + \not{q}_m^-) \gamma_\mu \not{q}_m^+ \gamma_\nu \right\} \\ \text{Tr} \left\{ \not{p}_M^- \Gamma_{NN\gamma}^\mu(q) \not{p}_M^+ \bar{\Gamma}_{NN\gamma}^\nu(q') (\not{k} - \not{p}_M^-) \bar{\Gamma}_{NN\gamma}^\sigma(k) \right\} \quad (104)$$

$$X_{24} = -\frac{e_p^3 e_e^3}{q^2 q'^2} \text{Tr} \left\{ \not{q}_m^- \gamma_\sigma (\not{k} + \not{q}_m^-) \gamma_\mu \not{q}_m^+ \gamma_\nu \right\} \\ \text{Tr} \left\{ \not{p}_M^- \Gamma_{NN\gamma}^\mu(q) \not{p}_M^+ \bar{\Gamma}_{NN\gamma}^\sigma(k) (\not{p}_M^+ - \not{k}) \bar{\Gamma}_{NN\gamma}^\nu(q') \right\} \quad (105)$$

$$X_{31} = -\frac{e_p^3 e_e^3}{q^2 q'^2} \text{Tr} \left\{ \not{q}_m^- \gamma_\mu \not{q}_m^+ \gamma_\sigma (-\not{k} - \not{q}_m^+) \gamma_\nu \right\} \\ \text{Tr} \left\{ \not{p}_M^- \Gamma_{NN\gamma}^\sigma(k) (\not{k} - \not{p}_M^-) \Gamma_{NN\gamma}^\mu(q') \not{p}_M^+ \bar{\Gamma}_{NN\gamma}^\nu(q) \right\} \quad (106)$$

$$X_{32} = -\frac{e_p^3 e_e^3}{q^2 q'^2} \text{Tr} \left\{ \not{q}_m^- \gamma_\mu \not{q}_m^+ \gamma_\nu (\not{k} + \not{q}_m^-) \gamma_\sigma \right\} \\ \text{Tr} \left\{ \not{p}_M^- \Gamma_{NN\gamma}^\sigma(k) (\not{k} - \not{p}_M^-) \Gamma_{NN\gamma}^\mu(q') \not{p}_M^+ \bar{\Gamma}_{NN\gamma}^\nu(q) \right\} \quad (107)$$

$$X_{33} = -\frac{e_p^4 e_e^2}{q'^4} \text{Tr} \left\{ \not{q}_m^- \gamma_\mu \not{q}_m^+ \gamma_\nu \right\} \\ \text{Tr} \left\{ \not{p}_M^- \Gamma_{NN\gamma}^\sigma(k) (\not{k} - \not{p}_M^-) \Gamma_{NN\gamma}^\mu(q') \not{p}_M^+ \bar{\Gamma}_{NN\gamma}^\nu(q') (\not{k} - \not{p}_M^-) \bar{\Gamma}_{\sigma NN\gamma}(k) \right\} \quad (108)$$

$$X_{34} = -\frac{e_p^4 e_e^2}{q'^4} \text{Tr} \left\{ \not{q}_m^- \gamma_\mu \not{q}_m^+ \gamma_\nu \right\} \\ \text{Tr} \left\{ \not{p}_M^- \Gamma_{NN\gamma}^\sigma(k) (\not{k} - \not{p}_M^-) \Gamma_{NN\gamma}^\mu(q') \not{p}_M^+ \bar{\Gamma}_{\sigma NN\gamma}(k) (\not{p}_M^+ - \not{k}) \bar{\Gamma}_{NN\gamma}^\nu(q') \right\} \quad (109)$$

$$X_{41} = -\frac{e_p^3 e_e^3}{q^2 q'^2} \text{Tr} \left\{ \not{q}_m^- \gamma_\mu \not{q}_m^+ \gamma_\sigma (-\not{k} - \not{q}_m^+) \gamma_\nu \right\} \\ \text{Tr} \left\{ \not{p}_M^- \Gamma_{NN\gamma}^\mu(q') (\not{p}_M^+ - \not{k}) \Gamma_{NN\gamma}^\sigma(k) \not{p}_M^+ \bar{\Gamma}_{NN\gamma}^\nu(q) \right\} \quad (110)$$

$$X_{42} = -\frac{e_p^3 e_e^3}{q^2 q'^2} \text{Tr} \left\{ \not{q}_m^- \gamma_\mu \not{q}_m^+ \gamma_\nu (\not{k} + \not{q}_m^-) \gamma_\sigma \right\} \\ \text{Tr} \left\{ \not{p}_M^- \Gamma_{NN\gamma}^\mu(q') (\not{p}_M^+ - \not{k}) \Gamma_{NN\gamma}^\sigma(k) \not{p}_M^+ \bar{\Gamma}_{NN\gamma}^\nu(q) \right\} \quad (111)$$

$$X_{43} = -\frac{e_p^4 e_e^2}{q'^4} \text{Tr} \left\{ \not{q}_m^- \gamma_\mu \not{q}_m^+ \gamma_\nu \right\} \\ \text{Tr} \left\{ \not{p}_M^- \Gamma_{NN\gamma}^\mu(q') (\not{p}_M^+ - \not{k}) \Gamma_{NN\gamma}^\sigma(k) \not{p}_M^+ \right. \\ \left. \bar{\Gamma}_{NN\gamma}^\nu(q') (\not{k} - \not{p}_M^-) \bar{\Gamma}_{\sigma NN\gamma}(k) \right\} \quad (112)$$

$$X_{44} = -\frac{e_p^4 e_e^2}{q'^4} \text{Tr} \left\{ \not{q}_m^- \gamma_\mu \not{q}_m^+ \gamma_\nu \right\} \\ \text{Tr} \left\{ \not{p}_M^- \Gamma_{NN\gamma}^\mu(q') (\not{p}_M^+ - \not{k}) \Gamma_{NN\gamma}^\sigma(k) \not{p}_M^+ \right. \\ \left. \bar{\Gamma}_{\sigma NN\gamma}(k) (\not{p}_M^+ - \not{k}) \bar{\Gamma}_{NN\gamma}^\nu(q') \right\} \quad (113)$$

When the photon is emitted by the hadrons or by the leptons, the hadronic and the leptonic tensors contain ten terms. The product of the traces is written

$$Y_{ij} = \sum_{k,k'=1}^{10} C_{ijk}^h C_{ijk'}^\ell T_H^{\mu\nu}(k) T_{L\mu\nu}(k') \quad (114)$$

The tensors $T_H^{\mu\nu}(k)$, $T_{L\mu\nu}(k')$ are given in Table 4

Table 4. Hadronic and Leptonic tensors I

k	$T_H^{\mu\nu}$	k'	$T_{L\mu\nu}$
1	$g^{\mu\nu}$	1	$g_{\mu\nu}$
2	$k^\mu k^\nu$	2	$k_\mu k_\nu$
3	$k^\mu p^{-\nu}$	3	$k_\mu q_\nu^+$
4	$k^\mu p^{+\nu}$	4	$k_\mu q_\nu^-$
5	$p^{-\mu} k^\nu$	5	$q_\mu^+ k_\nu$
6	$p^{-\mu} p^{-\nu}$	6	$q_\mu^+ q_\nu^+$
7	$p^{-\mu} p^{+\nu}$	7	$q_\mu^+ q_\nu^-$
8	$p^{+\mu} k^\nu$	8	$q_\mu^- k_\nu$
9	$p^{+\mu} p^{-\nu}$	9	$q_\mu^- q_\nu^+$
10	$p^{+\mu} p^{+\nu}$	10	$q_\mu^- q_\nu^-$

When the photon is emitted by a hadron and by a lepton, the hadronic and the leptonic tensors contain thirty six terms.

$$Y_{ij} = \sum_{k,k'=1}^{36} C_{ijk}^h C_{ijk'}^\ell T_H^{\mu\nu}(k) T_{L\mu\nu}(k') \quad (115)$$

with the tensors $T_H^{\mu\nu}(k)$, $T_{L\mu\nu}(k')$ given in Table 5.

Each coefficient C_{ijk}^h in the hadronic tensor depends on the electromagnetic form factors and its analytical expression has been derived with the help of Mathematica [28], but will not be given in this paper. A

numerical check, obtained in calculating numerically the hadronic and leptonic traces, has been done.

Table 5. Hadronic and Leptonic tensors II

k	$T_H^{\mu\nu\sigma}$	k'	$T_{L\mu\nu\sigma}$
1	$g^{\mu\nu} k^\sigma$	1	$g_{\mu\nu} k_\sigma$
2	$g^{\mu\nu} p^{-\sigma}$	2	$g_{\mu\nu} q_\sigma^+$
3	$g^{\mu\nu} p^{+\sigma}$	3	$g_{\mu\nu} q_\sigma^-$
4	$g^{\mu\sigma} k^\nu$	4	$g_{\mu\sigma} k_\nu$
5	$g^{\mu\sigma} p^{-\nu}$	5	$g_{\mu\sigma} q_\nu^+$
6	$g^{\mu\sigma} p^{+\nu}$	6	$g_{\mu\sigma} q_\nu^-$
7	$g^{\nu\sigma} k^\mu$	7	$g_{\nu\sigma} k_\mu$
8	$g^{\nu\sigma} p^{-\mu}$	8	$g_{\nu\sigma} q_\mu^+$
9	$g^{\nu\sigma} p^{+\mu}$	9	$g_{\nu\sigma} q_\mu^-$
10	$k^\mu k^\nu k^\sigma$	10	$k_\mu k_\nu k_\sigma$
11	$k^\mu k^\nu p^{-\sigma}$	11	$k_\mu k_\nu q_\sigma^+$
12	$k^\mu k^\nu p^{+\sigma}$	12	$k_\mu k_\nu q_\sigma^-$
13	$k^\mu p^{-\nu} k^\sigma$	13	$k_\mu q_\nu^+ k_\sigma$
14	$k^\mu p^{-\nu} p^{-\sigma}$	14	$k_\mu q_\nu^+ q_\sigma^+$
15	$k^\mu p^{-\nu} p^{+\sigma}$	15	$k_\mu q_\nu^+ q_\sigma^-$
16	$k^\mu p^{+\nu} k^\sigma$	16	$k_\mu q_\nu^- k_\sigma$
17	$k^\mu p^{+\nu} p^{-\sigma}$	17	$k_\mu q_\nu^- q_\sigma^+$
18	$k^\mu p^{+\nu} p^{+\sigma}$	18	$k_\mu q_\nu^- q_\sigma^-$
19	$p^{-\mu} k^\nu k^\sigma$	19	$q_\mu^+ k_\nu k_\sigma$
20	$p^{-\mu} k^\nu p^{-\sigma}$	20	$q_\mu^+ k_\nu q_\sigma^+$
21	$p^{-\mu} k^\nu p^{+\sigma}$	21	$q_\mu^+ k_\nu q_\sigma^-$
22	$p^{-\mu} p^{-\nu} k^\sigma$	22	$q_\mu^+ q_\nu^+ k_\sigma$
23	$p^{-\mu} p^{-\nu} p^{-\sigma}$	23	$q_\mu^+ q_\nu^+ q_\sigma^+$
24	$p^{-\mu} p^{-\nu} p^{+\sigma}$	24	$q_\mu^+ q_\nu^+ q_\sigma^-$
25	$p^{-\mu} p^{+\nu} k^\sigma$	25	$q_\mu^+ q_\nu^- k_\sigma$
26	$p^{-\mu} p^{+\nu} p^{-\sigma}$	26	$q_\mu^+ q_\nu^- q_\sigma^+$
27	$p^{-\mu} p^{+\nu} p^{+\sigma}$	27	$q_\mu^+ q_\nu^- q_\sigma^-$
28	$p^{+\mu} k^\nu k^\sigma$	28	$q_\mu^- k_\nu k_\sigma$
29	$p^{+\mu} k^\nu p^{-\sigma}$	29	$q_\mu^- k_\nu q_\sigma^+$
30	$p^{+\mu} k^\nu p^{+\sigma}$	30	$q_\mu^- k_\nu q_\sigma^-$
31	$p^{+\mu} p^{-\nu} k^\sigma$	31	$q_\mu^- q_\nu^+ k_\sigma$
32	$p^{+\mu} p^{-\nu} p^{-\sigma}$	32	$q_\mu^- q_\nu^+ q_\sigma^+$
33	$p^{+\mu} p^{-\nu} p^{+\sigma}$	33	$q_\mu^- q_\nu^+ q_\sigma^-$
34	$p^{+\mu} p^{+\nu} k^\sigma$	34	$q_\mu^- q_\nu^- k_\sigma$
35	$p^{+\mu} p^{+\nu} p^{-\sigma}$	35	$q_\mu^- q_\nu^- q_\sigma^+$
36	$p^{+\mu} p^{+\nu} p^{+\sigma}$	36	$q_\mu^- q_\nu^- q_\sigma^-$

C.2 Soft photon and factorization.

In this section, we show how the soft photon cross section factorizes in term of the Born cross section.

The product of the hadronic and leptonic tensors in the Born term is given by

$$Y_{00} = Tr \left\{ \not{p}_M^- \Gamma_{NN\gamma}^\mu(q) \not{p}_M^+ \bar{\Gamma}_{NN\gamma}^\nu(q) \right\} \\ Tr \left\{ \not{q}_m^- \gamma_\mu \not{q}_m^+ \gamma_\nu \right\} \quad (116)$$

When the photon energy goes to zero, we have:

$$\Gamma_{NN\gamma}^\sigma(k) \rightarrow \gamma^\sigma; \quad \bar{\Gamma}_{NN\gamma}^\sigma(k) \rightarrow \gamma^\sigma \quad (117)$$

$$q' = p^- + p^+ - k = q - k \rightarrow q \quad (118)$$

$$Y_{ij} \rightarrow Y_{ij}^{\text{Soft}} \quad (119)$$

We have seen in eq.(44) that there are ten terms which have a well definite limit when the photon energy goes to zero. So the factorization of the soft cross section in terms of the Born cross section can be studied through the quantities $-Y_{11}^{\text{Soft}}/4Y_{00}$ to $-(Y_{34}^{\text{Soft}} + Y_{43}^{\text{Soft}})/4Y_{00}$. In these quantities, the numerator and the denominator depend on the electromagnetic form factors. The derivation of these quantities has been done with the help of Mathematica [28]. The result is given in table 6.

Table 6. Ratio of soft photon cross section to Born cross section

Definition	Result
$-Y_{11}^{\text{Soft}}/4Y_{00}$	$-q^{+2}$
$-Y_{22}^{\text{Soft}}/4Y_{00}$	$-q^{-2}$
$-Y_{33}^{\text{Soft}}/4Y_{00}$	$-p^{-2}$
$-Y_{44}^{\text{Soft}}/4Y_{00}$	$-p^{+2}$
$-(Y_{12}^{\text{Soft}} + Y_{21}^{\text{Soft}})/4Y_{00}$	$2q^+ \cdot q^-$
$-(Y_{13}^{\text{Soft}} + Y_{31}^{\text{Soft}})/4Y_{00}$	$-2q^+ \cdot p^-$
$-(Y_{14}^{\text{Soft}} + Y_{41}^{\text{Soft}})/4Y_{00}$	$2q^+ \cdot p^+$
$-(Y_{23}^{\text{Soft}} + Y_{32}^{\text{Soft}})/4Y_{00}$	$2q^- \cdot p^-$
$-(Y_{24}^{\text{Soft}} + Y_{42}^{\text{Soft}})/4Y_{00}$	$-2q^- \cdot p^+$
$-(Y_{34}^{\text{Soft}} + Y_{43}^{\text{Soft}})/4Y_{00}$	$2p^- \cdot p^+$

The result is very interesting. It shows that each ratio is independent of the electromagnetic form factors. The sum of each term of the right column of the Table 6 divided by its corresponding propagator lead to the following analytical function:

$$F^{\text{Soft}} = - \left(\frac{p^+}{k \cdot p^+} - \frac{p^-}{k \cdot p^-} + \frac{q^-}{k \cdot q^-} - \frac{q^+}{k \cdot q^+} \right)^2 \quad (120)$$

The soft correction δ_{Soft} is obtained through the integration of this function over the photon variables (Eq.23).

References

1. A. J. R. Puckett et al., Phys. Rev. Lett. **104**, 242301 (2010) and references therein.
2. I. A. Qattan et al., Phys. Rev. Lett. **94**, 142301 (2005) and references therein.
3. J. Arrington, P. G. Blunden and W. Melnitchouk, arXiv:nucl-th/1105.0951.
4. P. A. M. Guichon and M. Vanderhaeghen, Phys. Rev. Lett. **91**, 142303 (2003).
5. M. P. Rekalo and E. Tomasi-Gustafsson, Nucl. Phys. A **742**, 322 (2004).
6. Y. C. Chen, A. Afanasev, S. J. Brodsky, C. E. Carlson and M. Vanderhaeghen, Phys. Rev. Lett. **93**, 122301 (2004).
7. C. E. Carlson and M. Vanderhaeghen, Annu. Rev. Nucl. Part. Sci. **57**, 171 (2007).
8. L. C. Maximon and J. A. Tjon, Phys. Rev. C **62**, 054320 (2000).
9. Yu. M. Bystritskiy, E. A. Kuraev and E. Tomasi-Gustafsson, Phys. Rev. C **75**, 015207 (2007).
10. P. G. Blunden, M. Melnitchouk and J. A. Tjon, Phys. Rev. Lett. **91**, 142304 (2003).
11. R. Baldini et al., Eur. Phys. J. C **46**, 421 (2006); S. Pacetti (private communication)
12. S. Pacetti, Chinese Phys. C **34**, 874 (2010)
13. G. Bardin et al., Nucl. Phys. B **411**, 3 (1994).
14. M. Ambrogiani et al., Phys. Rev. D **60**, 032002 (1999) and references therein.
15. M. Ablikim et al., Phys. Lett. B **630**, 14 (2005)
16. B. Aubert et al., Phys. Rev. D **73**, 012005 (2006).
17. M. Sudol et al., Eur. Phys. J. A **44**, 373 (2010).
18. A. I. Ahmadov, V. V. Bytev, E. A. Kuraev and E. Tomasi-Gustafsson, Phys. Rev. D **82**, 094016 (2010).
19. G. I. Gakh, N. P. Merenkov and E. Tomasi-Gustafsson, Phys. Rev. C **83**, 045202 (2011).
20. A. Zichichi, S. M. Berman, N. Cabibbo and R. Gatto, Nuovo Cimento **24**, 170 (1962)
21. F. Iachello and Q. Wan, Phys. Rev. C **69**, 055204 (2004).
22. E.C. Titchmarsh, Theory of functions (Oxford University Press, London 1939)
23. M. Vanderhaeghen, J.M. Friedrich, D. Lhuillier, D. Marchand, L. Van Hoorebecke, and J. Van de Wiele Phys. Rev. C **62**, 025501 (2000)
24. G. Bonneau and F. Martin, Nucl. Phys. B **27**, 381 (1971).
25. G. 't Hooft and M. Veltman, Nucl. Phys. B **153**, 365 (1979).
26. J. Guttman, N. Kivel and M. Vanderhaeghen, Phys. Rev. D **83**, 094021 (2011).
27. E. A. Kuraev and V. S. Fadin, Yad. Fiz. **41**, 733 (1985) [Sov. J. Nucl. Phys. **41**, 466 (1985)].
28. Wolfram Research, Inc., Mathematica, Version 8.0, Champaign, IL (2010)

Table 1. Soft and virtual corrections : $s = 5.4 \text{ GeV}^2$, $\omega = 12 \text{ MeV}$, $\omega/E_{e^+} \approx 1\%$

$\theta_{e^+} (deg.)$	δ_{vac}	δ_{vertex}^e	δ_{Soft}^e	δ_{vertex}^p	δ_{Soft}^p	δ_{box}	δ_{Soft}^{ep}	δ_{SV}^e	δ_{SV}^{ep}
30.	0.0305	-0.2602	-0.0147	0.0160	-0.0127	-0.0033	-0.0697	-0.2444	-0.3108
60.	0.0305	-0.2602	-0.0147	0.0147	-0.0127	-0.0020	-0.0365	-0.2444	-0.2789
90.	0.0305	-0.2602	-0.0147	0.0132	-0.0127	0.0000	0.0000	-0.2444	-0.2439
120.	0.0305	-0.2602	-0.0147	0.0147	-0.0127	0.0020	0.0365	-0.2444	-0.2059
150.	0.0305	-0.2602	-0.0147	0.0160	-0.0127	0.0033	0.0697	-0.2444	-0.1713

Table 2. Soft and virtual corrections : $s = 12.9 \text{ GeV}^2$, $\omega = 18 \text{ MeV}$, $\omega/E_{e^+} \approx 1\%$

$\theta_{e^+} (deg.)$	δ_{vac}	δ_{vertex}^e	δ_{Soft}^e	δ_{vertex}^p	δ_{Soft}^p	δ_{box}	δ_{Soft}^{ep}	δ_{SV}^e	δ_{SV}^{ep}
30.	0.0332	-0.2991	-0.0006	0.0113	-0.0314	-0.0112	-0.1169	-0.2595	-0.3965
60.	0.0332	-0.2991	-0.0006	0.0095	-0.0314	-0.0059	-0.0558	-0.2595	-0.3372
90.	0.0332	-0.2991	-0.0006	0.0062	-0.0314	0.0000	0.0000	-0.2595	-0.2847
120.	0.0332	-0.2991	-0.0006	0.0095	-0.0314	0.0059	0.0558	-0.2595	-0.2256
150.	0.0332	-0.2991	-0.0006	0.0113	-0.0314	0.0112	0.1169	-0.2595	-0.1627